Int. J. Multiphase Flow Vol 11, No. 5, pp. 593–606, 1985
Printed in Great Britain.

0301-9322/85 $3.00 + .00
Pergamon/Elsevier

HEAT TRANSFER AND INTERFACIAL DRAG IN COUNTERCURRENT STEAM–WATER STRATIFIED FLOW

H. J. KIM,† S. C. LEE‡ and S. G. BANKOFF§
Northwestern University, Evanston, IL 60201, U.S.A.

(*Received* 22 *August* 1983; *in revised form* 30 *January* 1985)

Abstract—Local condensation heat transfer coefficients and interfacial shear stresses have been measured for countercurrent stratified flow of steam and subcooled water in rectangular channels over a wide range of inclination angles (4–87°) at two aspect ratios. Dimensionless correlations for the interfacial friction factor have been developed that show that it is a function of the liquid Reynolds number only. Empirical correlations of the heat transfer coefficient, based upon the bulk flow properties, have also been set up for the whole body of data encompassing the different inclination angles and aspect ratios. These indicate that the Froude number as a dimensionless gas velocity is a better correlating parameter than the gas Reynolds number. As an alternative approach, a simple dimensionless relationship for the heat transfer coefficient was obtained by analogy between heat and momentum transfer through the interface. Finally, a turbulence-centered model has been modified by using measured interfacial parameters for the turbulent velocity and length scales, resulting in good agreement with the data.

1. INTRODUCTION

Condensation heat transfer in a direct-contact mode can be encountered in a variety of industrial applications, such as reflux condensers and tubular contactors. In recent years, the modeling of direct-contact heat transfer has been of central importance in connection with the safety analysis of nuclear reactor systems. During a postulated loss-of-coolant accident in a pressurized-water reactor, emergency core cooling water is injected into the pressure vessel through the cold legs in order to prevent overheating of the reactor core. The subcooled ECC water is then brought into contact with escaping steam, which is generated within the core, resulting in countercurrent flow of steam and water. A knowledge of the thermal–hydraulic interactions of this countercurrent flow is important for the quantitative prediction of the course of the accident.

Several experimental studies have been carried out on local condensation rates in direct-contact stratified two-phase flow over the years (Linehan 1968; Cook *et al.* 1981; Lim *et al.* 1981; Segev *et al.* 1981). As a result, a number of empirical correlations on the condensation heat transfer coefficient have been developed, particularly based upon local parameters of two-phase flow. Although a condensing two-phase flow is never fully developed, local flow properties are used as correlating parameters. In general, these correlations involve a power-law relationship for the liquid Prandtl number as well as the vapor and liquid Reynolds numbers, in recognition of the fact that the principal thermal resistance lies on the liquid side,

$$\mathrm{Nu} = n_1 \mathrm{Re}_G^{n_2} \mathrm{Re}_L^{n_3} \mathrm{Pr}^{n_4}, \qquad [1]$$

where Nu is the Nusselt number; n_1, n_2, n_3, n_4 are experimental constants; Re is the Reynolds number; subscripts G and L are vapor and liquid, respectively; Pr is the Prandtl number; and where the dimensionless parameters are defined as $\mathrm{Nu} = h\delta/k$, $\mathrm{Re} = W/\mu$ and $\mathrm{Pr} = \nu_L/\alpha_L$. Unfortunately, it is found that for similar ranges of the local Nusselt number, the

†Present address: Korea Advanced Energy Research Institute, Seoul, South Korea.
‡Present address: Assistant Professor, Department of Mechanical Engineering, Yeongnam University, Kyungsan, South Korea.
§Author to whom correspondence should be addressed.

coefficients in [1] vary considerably from one author to another. Here, h is the local heat transfer coefficient, δ is the mean water layer thickness (m), k is thermal conductivity (kW/m^2K), W is mass flow rate per unit width (kg/sm), μ is the viscosity (Ns/m^2), ν is the kinematic viscosity (m^2/s) and α is the thermal diffusivity (m^2/s).

As an alternative approach, the concept of a Reynolds flux has been employed in correlating local transfer properties in condensing flow by comparison with adiabatic transfer properties. For example, Linehan (1968) suggested that the interfacial shear stress in a condensing flow is augmented by an amount equal to the condensation rate multiplied by the average vapor velocity. Mickley *et al.* (1954) proposed a somewhat similar relationship between the heat transfer coefficients with and without mass transfer. Their equation was originally suggested for boundary layer flows with suction, but may be extended to two-phase flows with condensation at the moving interface. By analogy with momentum transfer, the two-phase heat transfer coefficient may be correlated in terms of the single-phase heat transfer coefficient and the Lockhart-Martinelli parameter (Lockhart & Martinelli 1949). This approach has been widely used in heat transfer in forced-convection boiling (Dengler & Addams 1956; Guerrieri & Talty 1956; Schrock & Grossman 1962). A similar correlation based on the analogy between the condensation-induced heat transfer and momentum transfer through the interface will be derived in this paper.

Although correlations based upon macroscopic flow properties are convenient, these may be of limited usefulness, because the heat transfer mechanism in stratified two-phase flow is basically governed by the presence of interfacial waves. These in turn affect the turbulent properties of the flow near the interface. Bankoff *et al.* (1978) correlated the heat transfer coefficient in condensing cocurrent two-phase flow by means of a power-law relationship involving the turbulent liquid Reynolds number and the liquid Prandtl number. This draws upon the analogy between heat and mass transfer at the interface, starting with turbulent gas absorption models that relate the mass transfer coefficient to the local turbulent properties (Theofanous *et al.* 1976). The analogy is reasonable because a single driving force in the liquid, due either to a concentration gradient or to a temperature difference, is dominant in the transport process. Thomas (1979) applied models of this type to a variety of flow configurations, including a vertical water jet impinging on the free surface from below, grid turbulence decaying in an open channel and recirculating flows generated by submerged horizontal jets. Success in this approach evidently depends upon the appropriate choice of turbulent length and velocity scales (Bankoff 1980; Jensen 1981).

The present study deals with measurements of interfacial shear stresses and local heat transfer coefficients in a countercurrent stratified flow of condensing steam and water, using rectangular channels. Two aspect ratios and three inclination angles have been employed. Dimensionless correlations for the interfacial friction factor and the heat transfer coefficient are developed, based upon the local flow properties. A simple dimensionless relationship for the heat transfer coefficient, by the analogy between heat and momentum transfer through the interface, is also derived. Finally, a turbulence-centered model for the countercurrent stratified steam–water flow is proposed, using interfacial parameters for the turbulent velocity and length scales.

2. EQUIPMENT AND MEASUREMENTS

The steam–water countercurrent flow contactor is made up of three sections, consisting of an upper and a lower plenum, together with a test section, as shown in figure 1. The test section is a rectangular channel ~2.1 m long and 0.38 m wide, and was designed to ensure reasonably two-dimensional stratified countercurrent flow. The aspect ratio can be changed by replacing the sidewalls. The distance between the water entrance and exit is 1.27 m. The upper and the lower plena were designed to ensure smooth entry and exit of steam and water. The test section has its own support system, which permits any inclination between 0 and

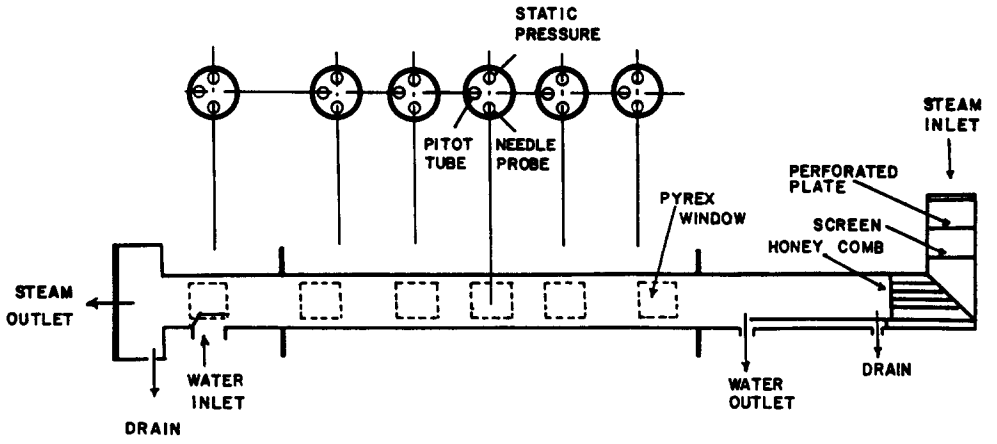

Figure 1. Sketch of test section.

90°. Two channel depths (H = 0.075 and 0.038 m) and three inclinations (θ = ~4, ~30 and ~90° from the horizontal) were employed.

The steam comes from the building supply, which is nominally saturated and at a pressure of 1.02 MPa. A steam separator and throttling valve ensure dry, superheated steam at the entrance to a manifold of flow-measurement venturis of either 3.18- or 5.08-cm diameter. The absolute pressure and temperature are monitored at the venturis to determine the thermodynamic condition of the incoming steam. When the steam enters the test section, a uniform flow is maintained by means of a perforated plate and honeycomb assembly in the lower plenum, and is then discharged at the top of the test section to the atmosphere. Normally the steam has 10–40°C superheat at the entrance and was assumed to be at atmospheric pressure for property calculations. The water loop includes two storage tanks, a heat exchanger, two circulating pumps and a 3.18-cm-diameter venturi. The water is introduced through a stainless-steel porous plate into the test section, and discharges by gravity through a fine-mesh screen in the lower plenum. A guide vane is used at the water entrance to maintain a smooth, uniform film. Hot water discharged from the test section is collected in a holding tank, whose water level is controlled by means of a bypass solenoid valve. The water inlet temperature can be regulated over the range of 1–98°C by varying the coolant rate in the heat exchanger.

The steam flow rates were measured at six stations along the channel centerline, whose location is given in table 1. The steam mass flow rate was obtained by integrating the measured steam velocity profile at each station, assuming two-dimensional flow. The two-dimensionality assumption was verified by pitot tube traverses across the width of the test section, and the integration method was checked by measuring the steam velocity profiles across the height of the test section with zero water flow. Upon comparing the measured inlet steam flow rate with the calculated local steam flow rate, it was found that the deviation was less than ±2%. The pitot tubes, which were electrically heated to prevent steam from condensing inside the tubes, were attached to a common traversing table,

Table 1. Geometry of test section

Data set	Inclination angle (θ)(°)	Width B(m)	Depth H(m)	Length L(m)	Aspect ratio, B/H	Measuring station (m), from steam inlet					
						1	2	3	4	5	6
A	4	0.38	0.075	1.27	5	0.26	0.44	0.62	0.80	0.98	1.27
B	30	0.38	0.075	1.27	5	0.26	0.44	0.62	0.80	0.98	1.27
C	87	0.38	0.075	1.27	5	0.22	0.40	0.58	0.76	0.93	1.27
D	33	0.38	0.038	1.27	10	0.22	0.40	0.58	0.76	0.93	1.27

allowing them to be positioned at selected elevations in the test section within 0.05 mm. The difference between total and static pressure for each pitot tube was measured by means of a diaphragm-type differential pressure transducer.

The temperatures of the steam and the water were measured with chromel–alumel thermocouples at the inlet and outlet. The probes are of the ungrounded junction type, enclosed within a 1.6-mm stainless-steel sheath, connected to a reference junction. The calibration of the thermocouples showed agreement to within ±1°C. Pressure taps 0.25 mm in diameter were located alongside the pitot tubes for pressure-drop measurements, from which the interfacial shear stress was calculated (Bankoff & Kim 1983). The mean water layer thickness was obtained by means of transversing micrometer-mounted conductivity probes. These consisted of a 0.5-mm stainless-steel needle with a sharpened tip, made nonwetting by the application of a Teflon coating, except at the very tip. A detailed description can be found in Bankoff & Kim (1983). The steam flow rate was calculated using the equation of state and the isentropic energy equation, based upon the measurements of thermodynamic state and pressure drop at the venturi. It showed agreement with the calibrated flow rate to within an accuracy of ±2%. The output signals were sampled and processed by a PDP-11/34 minicomputer, which is equipped with a 16-channel AR-11 A/D converter, a 16-channel DC amplifier and a CRT computer terminal located at the test site, with a usual sampling time and sampling frequency of 10 s and 240 Hz (5 s and 2000 Hz for the needle probe).

3. CORRELATION EQUATIONS

The heat transfer coefficient in the direct-contact mode may be defined as

$$h \triangleq \frac{i_{LG}}{(T_G - T_L)} \frac{dW_L}{dz}, \qquad [2]$$

where T_L and T_G are the temperatures (K) of the liquid and vapor, respectively, i_{LG} is the latent heat (kJ/kg); and dW_L/dz is the local condensation rate. Linehan (1968) proposed that the interfacial shear stress in the presence of condensation is dominated by the mass transfer, so that it can be expressed by

$$\tau_i = \tau_{i,a} + |(\bar{u}_G - u_i)| \frac{dW_L}{dz}, \qquad [3]$$

where τ_i and $\tau_{i,a}$ denote the interfacial shear stresses in condensing and adiabatic flow, respectively; $\bar{u}_G$ is the average velocity of the vapor; and u_i is the velocity of the interface. Upon eliminating the condensation rate from [2] and [3], one obtains a modified Reynolds-analogy equation,

$$\frac{\mathrm{St}}{\frac{1}{2}(f_i - f_{i,a})} = \frac{1}{\mathrm{Ja}}, \qquad [4]$$

where the dimensionless parameters are defined as

$$f \triangleq \frac{\tau}{\frac{1}{2}\rho_G(\bar{u}_G - u_i)^2} \qquad [5]$$

$$\mathrm{St} \triangleq \frac{h}{\rho_L C_{pL} |(\bar{u}_G - u_i)|} \qquad [6]$$

$$\mathrm{Ja} \triangleq \frac{\rho_L C_{pL}(T_G - T_L)}{\rho_G i_{LG}}. \quad [7]$$

In [4], $(f_i - f_{i,a})$ is the friction factor increment, which reflects the increase in the interfacial shear stress due to condensation. The Jakob number (Ja), which represents the capability of a liquid volume to absorb the latent heat of an equal volume of vapor released on condensation, results in a natural modification of the Reynolds analogy for single-phase flow [Stanton number (St) $= f/2$].

It was mentioned earlier that the coefficients of [1], a power-law relationship of the dimensionless bulk flow parameters, are inconsistent, varying from one author to another. This inconsistency appears to be associated with the selection of the gas Reynolds number as a dimensionless parameter when considering the effect of the vapor flow. A dimensionless relative gas velocity may be a more appropriate parameter than the gas Reynolds number to characterize the interfacial wave structure, which greatly affects the turbulent intensity near the interface, as well as the available heat transfer area. Hence, the Froude number (Fr), based on the relative velocity defined by [8], is used in correlating the local Nusselt number in the present study:

$$\mathrm{Fr} \triangleq \frac{|(\bar{u}_G - u_i)|}{\sqrt{g(H - \delta)}}. \quad [8]$$

As will be seen later, the replacement of the conventional gas Reynolds number by the Froude number results in a better correlation for unifying the whole set of data obtained under various geometrical conditions.

An attempt to correlate the heat transfer coefficient in terms of turbulent properties has been also made by analogy with heat and mass transfer. The turbulent Nusselt (Nu_t) and liquid Reynolds (Re_t) numbers in the turbulence-centered model (Thomas 1979; Bankoff 1980) can be defined by

$$\mathrm{Nu}_t = \frac{h\lambda_t}{k_L}, \quad [9]$$

$$\mathrm{Re}_t = \frac{u_t \lambda_t}{\nu_L}, \quad [10]$$

where λ_t and u_t are turbulent length and velocity scales, respectively. Considering the strong effect of the sheared and disturbed interface on the turbulent properties in countercurrent flow, the turbulent velocity and length scales may be defined in terms of interfacial parameters as follows:

$$u_t = \sqrt{\tau_i/\rho_L}, \quad [11]$$

$$\lambda_t = \delta. \quad [12]$$

The turbulent Nusselt number becomes identical to the Nusselt number in [1] by choosing $\lambda_t = \delta$. However, the turbulent Reynolds number defined by [10] represents a combined effect of both vapor and liquid flow by choosing the interfacial friction velocity as the velocity scale.

4. RESULTS AND DISCUSSION

4.1 *Presentation of typical data*

The experimental parameter ranges performed at various inclination angles and aspect ratios in the present study are summarized in table 2. The range of test conditions was

Table 2. Experimental flow range

Data set	θ (°)	B/H	Re_G	Re_L
A	4	5	2500–30,000	800–15,000
B	30	5	5000–30,000	1000– 8000
C	87	5	3000–20,000	800– 7000
D	33	10	3000–18,000	800– 5000

restricted for two reasons: (i) High water and/or steam flow rates produce slug formation and bridging, leading to countercurrent flow limitation or flooding; (ii) With highly subcooled water and low steam flow rates, complete condensation occurs inside the test section, resulting in the generation of large pressure pulses. Details on these instabilities have been reported in Lee & Bankoff (1983, 1984).

Typical data on steam flow rates at mixed steam inlet flow rate and water inlet temperature are shown in figure 2, together with curves obtained by fitting a fourth-order polynomial to the data. The data were collected at an inclination angle to the horizontal $\theta = 4°$ and aspect ratio $B/H = 5$ [where B is the channel width (m)]. As expected, the condensation rate increases with increasing water flow rate. However, it is interesting to note that for $m_{L,in} = 0.4$ kg/s, the slope of the curve is maximum (indicating that the heat transfer coefficient is greatest) near the steam exit, whereas the maximum occurs near the steam entrance for $m_{L,in} = 1.61$ kg/s. This shows the dominant effect of the agitated interface on the heat transfer mechanism at high water flow rates.

Shear stress data collected at $\theta = 4°$ and $B/H = 5$ are shown in figure 3. The interfacial shear stress was calculated from the integral momentum balance, using measured steam flow rates, pressure gradients and water-layer thickness (Kim & Bankoff 1983). The interfacial shear stress increases with increasing steam and liquid flow rates, along with the condensation rate. However, the effect of the vapor flow rate appears to be the more significant, because the interfacial shear stress induced by condensation dominates that owing to the interface roughness. Axial heat transfer coefficient profiles for various inlet steam flow rates, inclination angles and aspect ratios are shown in figures 4 and 5, respectively. It is evident from figure 4 that the local heat transfer coefficient is significantly

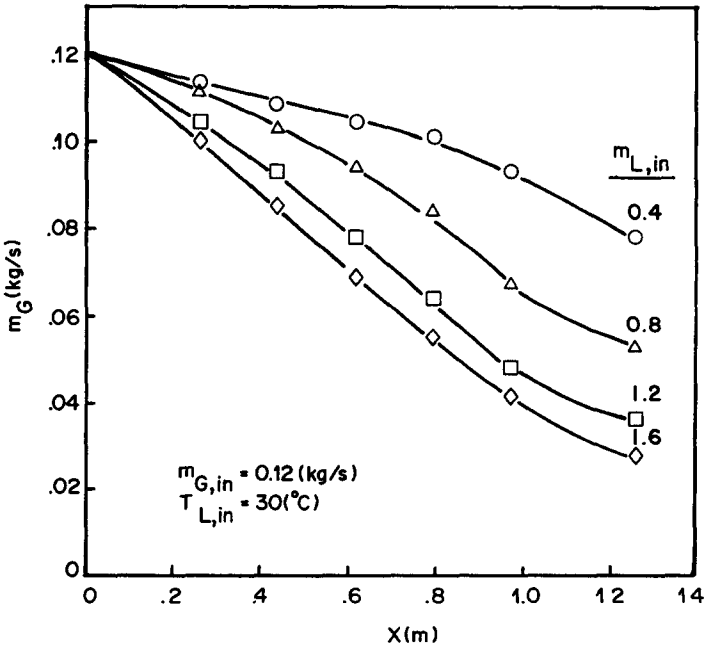

Figure 2. Axial steam flow rate profiles as a function of inlet water flow rate.

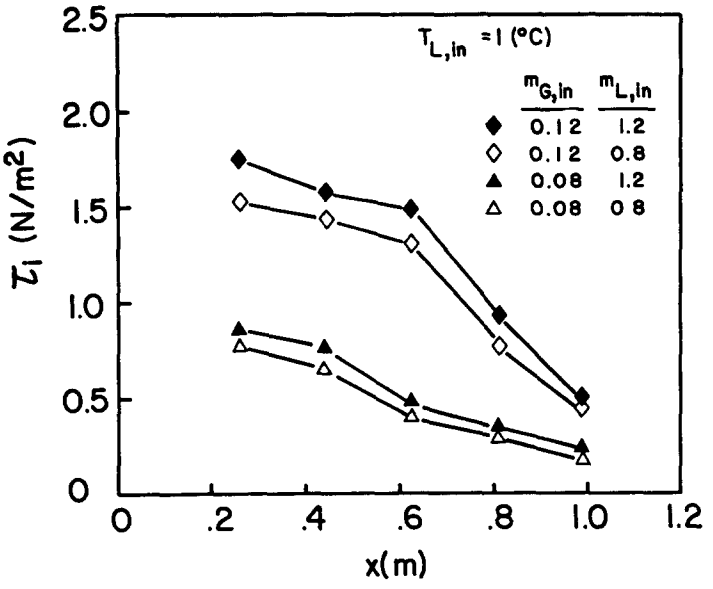

Figure 3. Axial distribution of interfacial shear stress as a function of inlet flow conditions.

affected by the steam inlet flow rate. Figure 5 shows a strong dependence of the coefficient upon the aspect ratio and the inclination angle. Under the same bulk flow conditions, the heat transfer coefficient tends to increase as the inclination angle increases. This can be attributed to the increase in the effective roughness of the interfacial waves and turbulent mixing near the interface (Kim 1983). A change of the aspect ratio with the same entrance mass flow rates results in significant change of the heat transfer coefficient, as seen in figure 5. This result confirms the validity of using the dimensionless relative vapor velocity in

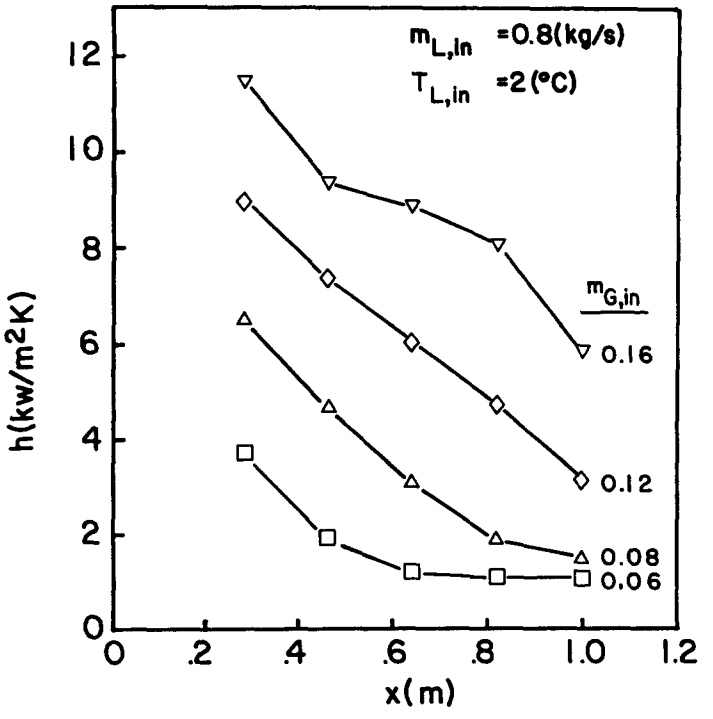

Figure 4. Axial heat transfer coefficient profiles as a function of inlet steam flow rate.

	A	B	C	D
θ (°)	4	30	87	33
B/H	5	5	5	10

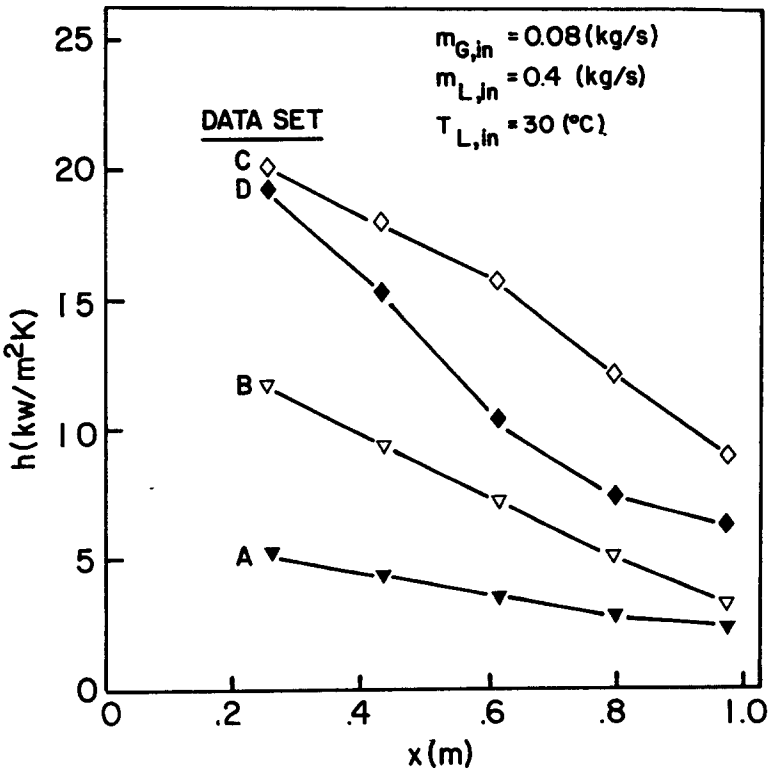

Figure 5. Axial heat transfer coefficient profiles as a function of inclination angle and aspect ratio. Data sets same as in figure 4.

correlating the local Nusselt number in a power-law relationship, such as [1], since the change does not affect the gas Reynolds number.

4.2 *Interfacial friction factor*

Correlations of the interfacial friction factor based upon the bulk flow properties have been developed for nearly horizontal ($\theta = 4°$) and nearly vertical ($\theta = 87°$) countercurrent steam–saturated water flows. It was found that the interfacial friction factor for the three-dimensional wave regime is dependent only upon the liquid Reynolds number at both inclinations. This is consistent with the experimental results of other investigators (Linehan 1968; Takahama *et al.* 1974; Theofanous *et al.* 1975). By contrast, for the roll-wave regime, it was reported that the friction factor is strongly dependent upon the gas as well as the liquid Reynolds number (Lee & Bankoff 1983). This seems to be reasonable because the dependence of the gas flow on the interfacial wave parameters, such as the mean water layer thickness, wave amplitude and frequency, is insignificant in the three-dimensional wave regime, whereas the crest height and frequency of the roll waves superimposed on the three-dimensional waves increase with increasing gas flow rate (Kim 1983; Lee 1983). The correlations for the adiabatic interfacial friction factor obtained by a least-squares routine give

$$f_{i,a} = a\,\mathrm{Re}_L + b, \qquad [13]$$

where $a = 0.14 \times 10^{-5}$ and $b = 0.021$ for the nearly horizontal flow and $a = 0.16 \times 10^{-5}$ and $b = 0.025$ for the nearly vertical flow. These correlations are comparable with the Linehan correlation, giving $a = 0.23 \times 10^{-5}$ and $b = 0.0131$ for horizontal cocurrent air–water flow. A comparison of these correlations with several sets of experimental data is shown in figure 6. It is interesting to note that the direction of the gas flow does not alter the magnitude of the

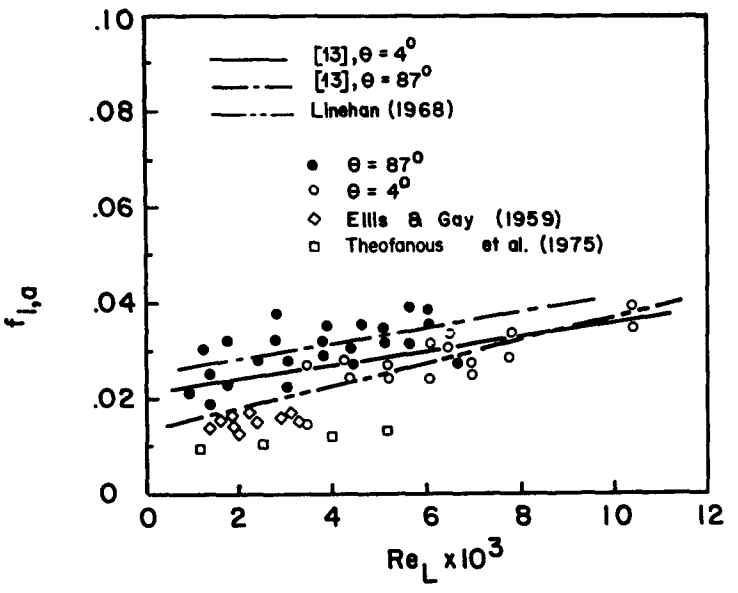

Figure 6. Comparison of adiabatic friction factor correlations with experimental data.

friction factor significantly in nearly horizontal or horizontal flow. However, the interfacial friction factors in nearly vertical flow increase by ~20% compared with those in nearly horizontal flow over the practical range of liquid Reynolds numbers. The data for cocurrent horizontal flow without interfacial mass transfer according to Ellis & Gay (1959) and Theofanous *et al.* (1975) are lower than the present nearly horizontal countercurrent condensing flow friction factors, as might be expected.

4.3 *Local heat transfer coefficients*

The local Nusselt number can be considered to be principally a function of the local liquid Reynolds number, the gas Froude number and the liquid Prandtl number. As noted above, the gas Reynolds number in the conventional equation, i.e. [1], was replaced by the Froude number to take into account the thickness of the gas and liquid layers. A least-squares fit of the entire body of data results in

$$Nu = 0.966 \times 10^{-3} Re_L^{0.98} Pr^{0.95} Fr^{0.8}. \quad [14]$$

Here, the average vapor velocity was chosen as a characteristic velocity in the Froude number for calculation purposes, since the interface velocity u_i in [8] is much smaller than $\bar{u}_G$ in this countercurrent two-phase flow. Equation [14] includes the effect of the aspect ratio implicity through the Froude number. From the definition of the Froude number, the following relationship can be obtained:

$$Fr^{1/2} = \nu_G (H - \delta)^{-3/2} g^{-1/2} Re_G. \quad [15]$$

This equation indicates that at a fixed gas Reynolds number (therefore at a fixed steam mass flow rate, according to the definition of the Reynolds number), a decrease in the aspect ratio results in an increase of the Froude number, and thus of the heat transfer coefficient. This result agrees with the experimental data shown in figure 5. The effect of the inclination angle can be also deduced from this correlation. For a given flow condition, the heat transfer coefficient increases as the water-layer thickness decreases (or, equivalently, the inclination angle increases), since the effect of the water-layer thickness is included in the local Nusselt number. A comparison of the measured Nusselt number with [14] is shown in figure 7. The

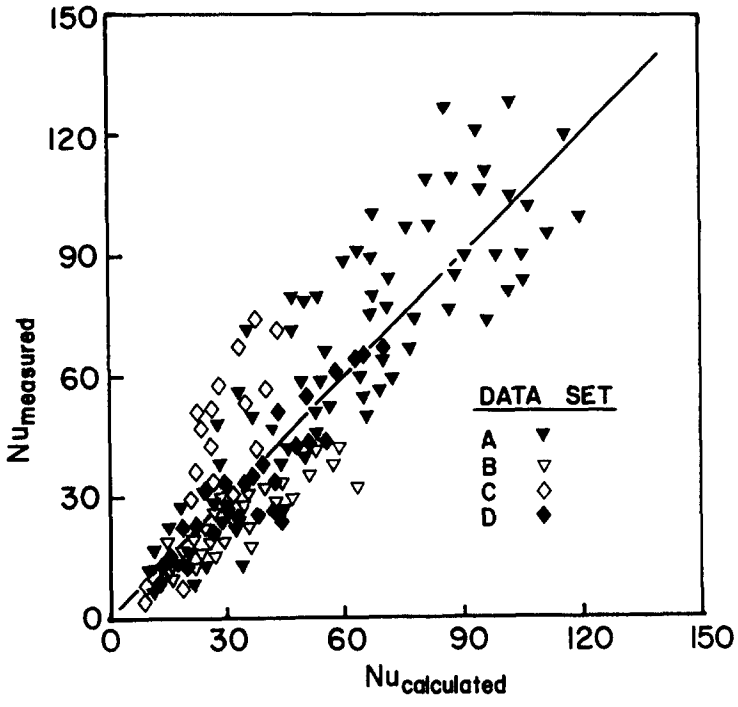

Figure 7. Comparison of measured Nusselt number with the calculated value [14].

nearly vertical flow data show a steeper trend, as might be expected, with increasing water or steam flow rates (and hence increasing Nusselt number) than the flow in which gravity acts more effectively to suppress wave growth.

Figure 8 shows a comparison of the present correlation with the experimental data of Segev *et al.* (1981) and Cook *et al.* (1981). The present correlation corresponds to the Cook *et al.* data over a reasonable range, but the Segev *et al.* data are lower than the calculated values. Some differences in technique of the two sets of experiments may account for this discrepancy. The present (also Cook *et al.*) heat transfer coefficient data were obtained by direct measurements of local condensation rates, whereas Segev *et al.* estimated the heat

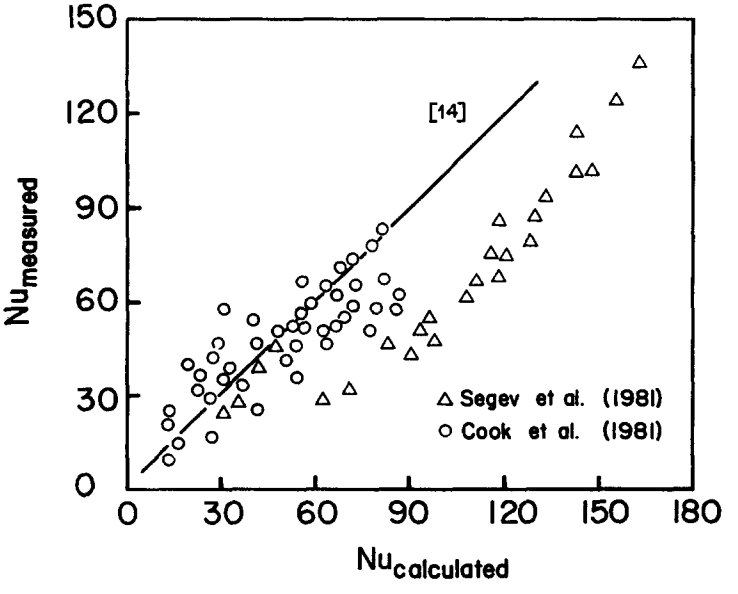

Figure 8. Comparison of Segev *et al.* (1981) and Cook *et al.* (1981) data with present correlation.

transfer coefficients by measuring the wall surface temperatures with the assumption of a uniform temperature profile across the liquid film. The wall surface temperatures are smaller than, or at most the same as, the bulk water temperatures, even for turbulent liquid films. Because of the wider range of inclination angle and aspect ratio, the present correlation [14] is tentatively recommended over the Segev *et al.* correlation.

As an alternative approach, a simple correlation by analogy between heat and momentum transfer has been sought, based upon [4]. The measured interfacial friction factors f_i were compared with the adiabatic interfacial friction factor $f_{i,a}$ calculated from [13]. The results showed that $f_{i,a}$ is much smaller than f_i, except for relatively low liquid subcooling. This suggests that the momentum transfer through the interface is controlled mainly by the condensation mass transfer, rather than form drag. Therefore, following the Reynolds analogy for single-phase flow, a simple approximation is

$$f_i - f_{i,a} = Cf_i, \qquad [16]$$

where the constant C was estimated to be 0.754 by a least-squares fit to the present data. This approximation is reasonable because in most practical cases, the water outlet temperature is not expected to reach the saturation value in the three-dimensional wave region. A comparison of this correlation with the present data is shown in figure 9. It is seen that most of the data lie within a ±20% error range of the correlation.

4.4 *Turbulence-centered model*

The turbulent heat transfer equation deduced from the gas-absorption model (Theofanous *et al.* 1976) may be written as

$$\mathrm{Nu}_t = n_1 \mathrm{Re}_t^{n_2} \mathrm{Pr}_t^{n_3}, \qquad [17]$$

where the coefficients n_1–n_3 are determined empirically. It should be pointed out that [4] and [17] have a common feature in that the interfacial friction is used as a correlating parameter. By least-squares linear regression, n_3 was found to be 0.465 ± 0.045 with a 95% confidence limit. However, it was adjusted to 0.5, following Bankoff (1980) and Jensen (1981), because of the limited range of Prandtl numbers in the present tests. The exponent n_2 was found to

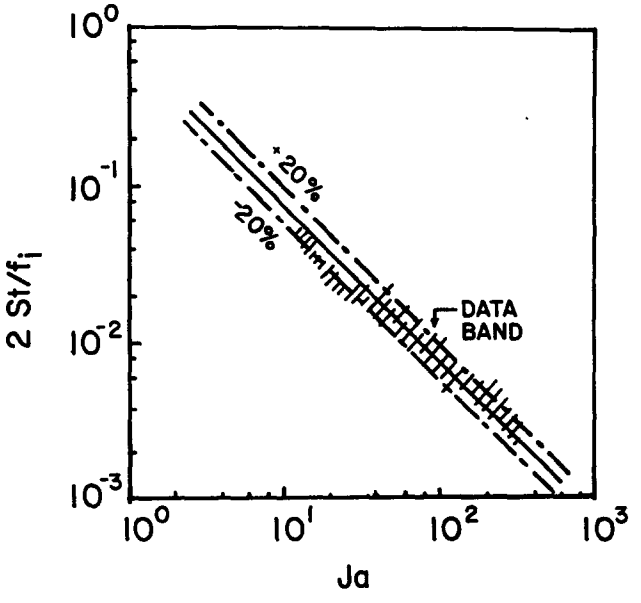

Figure 9. Comparison of data with improved heat transfer coefficient relationship.

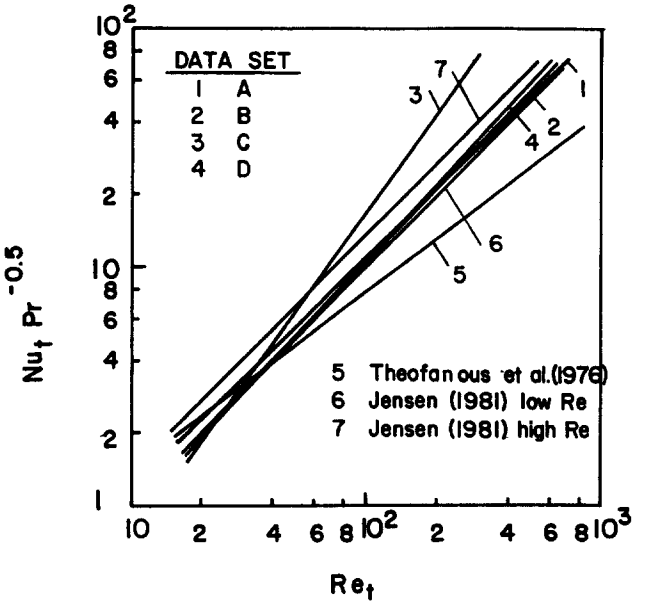

Figure 10. Comparison with other results for turbulence-centered model. Data sets same as in figure 4.

increase with the inclination angle, while it is nearly independent of the aspect ratio. The result shows that

$$n_1 = 0.0141 - 0.111\ (\sin\theta)^{0.93}, \qquad [18]$$

$$n_2 = 0.96 + 0.425\ (\sin\theta)^{2.2}. \qquad [19]$$

By extrapolating the coefficients in horizontal countercurrent flow ($\theta = 0$) from [18] and [19], one can obtain $n_1 = 0.141$ and $n_2 = 0.96$. These coefficients are almost identical to the results of Jensen (1981), who suggested the following numbers based on an examination of extensive data in horizontal concurrent flow: $n_1 = 0.14$ and $n_2 = 1.0$ for high liquid Reynolds numbers,† $n_1 = 0.1$ and $n_2 = 1.0$ for low liquid Reynolds numbers. This may not be surprising, partly because the interfacial waves in horizontal flow have a very similar structure, regardless of the direction of the gas flow (Lee 1983), and also because the correlations are based upon the local properties of the interfacial wave. The present correlation indicates a stronger effect of the turbulent Reynolds number, compared to the smooth-interface eddy-cell models proposed by Theofanous *et al.* (1976), who suggested $n = \frac{1}{2}$ or $\frac{3}{4}$ depending upon the range of the turbulent Reynolds number.‡ This is reasonable, however, since the influence of the gas Reynolds number, which is crucial for the rough interfaces, appears only in the length and velocity scales. This implies, in turn, a larger Reynolds number exponent. A comparison of the present correlation with other results is shown in figure 10.

5. CONCLUDING REMARKS

1. Empirical correlations [13] of the interfacial friction factor have been proposed. The friction factor was found to be dependent upon the liquid Reynolds number only in the three-dimensional wave regime.

2. An empirical correlation [14] of the heat transfer coefficient has been suggested in terms of easily accessible parameters for practical purposes. The Froude number as a

†This Reynolds number is defined by $Re_L = \bar{u}_L\, z/\nu_L$; where z is the distance from the water inlet (m).
‡The transition takes place at Re = 500.

dimensionless gas velocity was found to be a better correlating parameter than the gas Reynolds number. As an alternative approach, a simple heat transfer coefficient relationship ([4] and [16]) was obtained by the analogy between heat and momentum transfer through the interface.

3. A turbulence-centered model was modified by using measured interfacial parameters for the turbulent velocity and length scales. An improved correlation [17]–[19] was suggested and compared with other results.

Acknowledgement—This work was supported by a grant from the U.S. Nuclear Regulatory Commission.

REFERENCES

BANKOFF, S. G. 1980. Some condensation studies pertinent to LWR safety. *Int. J. Multiphase Flow* **6**, 51–67.

BANKOFF, S. G. & KIM, H. J. 1983 Local condensation rates in nearly horizontal stratified countercurrent flow of steam and cold water. *AIChE Symposium Series* **79**, 209–223.

BANKOFF, S. G., TANKIN, R. S. & YUEN, M. C. 1978 Local condensation rates in steam water mixing. Specialists Meeting on Transient Two Phase Flow, OECD Nuclear Energy Agency, Paris, France.

COOK, D., BANKOFF, S. G., TANKIN, R. S. & YUEN, M. C. 1981 Countercurrent steam-water flow in a vertical channel. NUREG/CR-2056.

DENGLER, C. E. & ADDAMS, J. N. 1956 Heat transfer mechanism for vaporization of water in a vertical tube. *AIChE Symposium Series* **52**, 95–103.

ELLIS, S. R. M. & GAY, G. 1959 The parallel flow of two fluid streams: interfacial shear and fluid-fluid interactions. *Trans. Inst. Chem. Engrs* **37**, 206–213.

GUERRIERI, S. A. & TALTY, R. D. 1956 A study of heat transfer to organic liquids in single tube, natural circulation vertical tube boilers. *AIChE Symposium Series* **52**, 69–77.

JENSEN, R. J. 1981 Interphase transport in horizontal stratified cocurrent flow. Ph.D. dissertation, Department of Mechanical Engineering, Northwestern University, Evanston, IL.

KIM, H. J. 1983 Local properties of countercurrent stratified stream-water flow. Ph.D. dissertation, Department of Mechanical Engineering, Northwestern University, Evanston, IL.

KIM, H. J. & BANKOFF, S. G. 1983 Local heat transfer coefficients for condensation in stratified countercurrent steam-water flows. *J. Heat Transfer* **105**, 706–712.

LEE, S. C. 1983 Stability of steam-water countercurrent stratified flow. Ph.D. dissertation, Department of Mechanical Engineering, Northwestern University, Evanston, IL.

LEE, S. C. & BANKOFF, S. G. 1983 Stability of steam-water countercurrent flow in an inclined channel: flooding. *J. Heat Transfer* **105**, 713–718.

LEE, S. C. & BANKOFF, S. G. 1984 Parametric effects on the onset of flooding in flat-plate geometries. *Int. J. Heat Mass Transfer* (in press).

LIM, I. S., BANKOFF, S. G., TANKIN, R. S. & YUEN, M. C. 1981 Cocurrent steam/water flow in a horizontal channel. NUREG/CR-2289.

LINEHAN, J. H. 1968 The interaction of two-dimensional stratified, turbulent air-water and steam-water flows. Ph.D. dissertation, Department of Mechanical Engineering, University of Wisconsin, Madison, WI.

LOCKHART, R. W. & MARTINELLI R. C. 1949 Proposed correlation of data for isothermal two-phase two-component flow in pipes. *AIChE Symposium Series* **45**, 39–48.

MICKLEY, H. S., ROSS, R. C., SQUYERS, A. L. & STEWART, W. E. 1954 Heat, mass, and momentum transfer for flow over a flat plate with blowing or suction. NACA-TN3208.

SCHROCK, V. E. & GROSSMAN, L. M. 1962 Forced convection boiling in tubes. *Nucl. Sci. Engn.* **12,** 474–480.

SEGEV, A., FLANIGAN, L. J., KURTH, R. E. & COLLIER, R. P. 1981 Experimental study of countercurrent steam condensation. *J. Heat Transfer* **103,** 307–311.

TAKAHAMA, H., FUJITA, H., KODAMA, T., KURIBAYASHI, M. & AISO, T. 1974 Heat and mass transfer in countercurrent flow of air and water film in a rectangular vertical duct. *Bull. JSME* **17,** 928–935.

THEOFANOUS, T. G., HOUZE, R. N. & JOHNS, D. M. 1975 Horizontal, stratified gas-liquid flow: the interfacial region. *AIChE Symposium on Heat Transfer,* San Francisco, CA.

THEOFANOUS, T. G., HOUZE, R. N. & BRUMFIELD, L. K. 1976 Turbulent mass transfer at free gas-liquid interfaces, with application to open-channel, buble and jet flows. *Int. J. Heat Mass Transfer* **19,** 613–624.

THOMAS, R. M. 1979 Condensation of steam on water in turbulent motion. *Int. J. Multiphase Flow* **5,** 1–15.